Numerical reconstruction of time-dependent thermal conductivity for heat equation from non-local overdetermination conditions

Mohammed Sabah Hussein
University of Baghdad, College of Science, Department of Mathematics, Baghdad, Iraq
mmmsh@scbaghdad.edu.iq

***Abstract*:** Recovery of time-dependent thermal conductivity has been numerically investigated. The problem of identification in one-dimensional heat equation from Cauchy boundary data and mass/energy specification has been considered. The inverse problem recasted as a nonlinear optimization problem. The regularized least-squares functional is minimised through *lsqnonlin* routine from MATLAB to retrieve the unknown coefficient. We investigate the stability and accuracy for numerical solution for two examples with various noise level and regularization parameter.

Keywords: Inverse problem; Finite difference method; nonlinear optimization, heat equation, regularization, coefficient identification problem.

1. Introduction

The concept of so-called inverse/backward problems have been dominated the research in late twentieth century due to wide range of applications; such as in engineering, geo- physics, economics and ecology [1].

During the consideration of inverse problems, the choice of overdetermination/additional conditions play an important role in the proofing the existence and uniqueness of the solution for example see, [2, 3, 4].

We investigate the numerical reconstruction of time-dependent thermal conductivity with respect to initial and non-homogeneous Dirichlet boundary conditions. Whilst, the overdetermination conditions are the energy/mass specification and the heat flux difference.

The organization of the paper as follows. In next section, the mathematical formulation and the unique solvability conditions are stated. In Section 3, the Crank-Nicolson FDM scheme for the direct problem has been presented and developed [5]. While, in Section 4 we consider the numerical solutions for inverse problems based on finding the quasi-solution for associated nonlinear optimization problem. Section 5, devoted to the numerical results and discussion. Finally, the conclusions are highlighted in Section 6.

2. Mathematical formulation

Consider the fixed parameters h > 0 and T > 0 which represent the length of a finite slab and time, respectively. The solution domain denoted by

$$D=\{(x,t): 0<x<h;\ 0<t\leq T\}.$$

In this paper, we consider the heat equation of the form

$$u_t = a(t)u_{xx} \qquad (x,t) \in D \qquad (1)$$

where $a(t) > 0$ is coefficient and $u(x, t)$ is the temperature. The heat capacity is taken to be unity and therefore the coefficient a(t) represent the time-dependent thermal conductivity. Equation (1) has to be solved subject to initial condition

$$u(x,0) = \varphi(x) \qquad 0 \leq x \leq h \qquad (2)$$

and nonhomogeneous Dirichlet boundary conditions

$$u(0,t) = \mu_1(t) \quad u(h,t) = \mu_2(t) \quad 0 \leq t \leq T \qquad (3)$$

If the coefficient a is given the equations (1)–(3) formulate a direct Dirichlet problem for finding the unknown temperature $u(x,t)$. The outputs of interest which should be computed are energy/mass specification

$$\int_0^h u(x,t)dx = \mu_3(t) \qquad 0 \leq t \leq T \qquad (4)$$

and the difference of heat flux at the ends

$$u_x(h,t) - u_x(0,t) = \mu_4(t) \quad 0 \leq t \leq T \qquad (5)$$

If conductivity coefficient a is unknown, in this case, an inverse problem for coefficient identification should be solved.

The problem for identifying the coefficient a(t) has been considered in [6] with periodic boundary conditions and nonlocal overspecified data. In this paper, the consideration has been given to recovery the unknown coefficient under

different boundary and overdetermination conditions as in equations (4) and (5). The unique solvability theorems for theses inverse problems are stated in the next subsections

2.1 Inverse problem 1 (IP1)

The IP1 requires determination of thermal conductivity a(t) > 0 together with the temperature u(x, t) satisfying the equations (1)–(4).

The unique solvability for IP1 was established in [7].

Theorem 1. *The inverse problem (1)–(4) is uniquely solvable if* $\varphi(x) \in C^1[0, h]$, $\mu_i(t) \in C^1[0, T]$, $i = 1, 2$, $\varphi'(h - x) - \varphi'(x) \geq 0$ *on* $[0,h/2]$, $\mu_1'(t) + \mu_2'(t) \geq 0$ *on* $[0, T]$ *and at least one of the functions* $\mu_1'(t) + \mu_2'(t)$ *and* $\varphi'(h - x) - \varphi'(x)$ *is not identically zero.*

Remark: notice that by differentiating equation (4) with respect to *t* and invoke (1) we have

$$\mu'_3(t) = \int_0^h u_t(x,t)dx = \int_0^h a(t)u_{xx}(x,t)dx \qquad (6)$$

after simple manipulation we obtain

$$a(t) = \frac{\mu'_3(t)}{u_x(h,t) - u_x(0,t)}, \qquad 0 \leq t \leq T, \qquad (7)$$

at $t = 0$

$$a(0) = \frac{\mu'_3(0)}{\varphi'(h) - \varphi'(0)}, \qquad (8)$$

provided that $\varphi'(h) - \varphi'(0) \neq 0$.

2.2 Inverse problem 2 (IP2)

The IP2 requires to solve the equations (1)–(3) and (5). Also, the unique solvability for IP2 was established in [7] and reads as follows.

Theorem 2. *Assume that the following conditions are satisfied*

1. $\mu_i \in C^1[0,T]$, i=1,2,4, $\varphi(x) \in C^2[0,h]$, $\varphi(0)+\varphi(h)=\mu_1(0)+\mu_2(0)$ and $\varphi'(h)-\varphi'(0) = \mu_4(0)$;
2. $\mu'_i(t)>0$, i=1,2, $\mu_4(t)\geq 0$ for $t\in[0,T]$, $\varphi''(x)>0$ on $[0,h]$.

Then the inverse problem (1)–(3) and (5) possesses a solution.

Theorem 3. *Assume that the functions* $\varphi(x)$ *and* $\mu_4(t)$ *satisfy the conditions*

1. $\varphi(x) \in C^2[0,h]$, $\mu_4(t) \in C^1[0,T]$, $\varphi''(x) \geq 0$ on $[0,h]$ and $\mu'_4(t)$ on $[0,T]$;
2. at least one of the functions $\varphi''(x)$ and $\mu'_4(t)$ is not identically zero.

Then the solution of the inverse problem (1)–(3) and (5) is unique.

3. Direct problem

In this section, consider numerical solution for the direct initial boundary value problem given by equation (1)–(3). The Finite difference method (FDM) with Crank-Nicolson scheme [5], has been employed which is unconditionally stable and second-order accurate in space and time. In order to employ this scheme, denote $u(x_i,t_j) := u_{i,j}$ and $a(t_j) := a_j$, where $x_i = i\Delta x$ and $t_j = j\Delta t$, $\varphi(x_i)=\varphi_i$, $\mu_k(t_j)=\mu_{kj}$,for k=1,2,3,4, i=0,M, j=0,N, $\Delta x=h/M$ and $\Delta t=T/N$.

Considering the heat equation (1), the Crank-Nicolson method, discretise (1)–(3) as

$$\frac{u_{i,j+1} - u_{i,j}}{\Delta t} = \frac{1}{2}\left(a_{j+1}\frac{u_{i+1,j+1} - 2u_{i,j+1} + u_{i-1,j+1}}{(\Delta x)^2} + a_j\frac{u_{i+1,j} - 2u_{i,j} + u_{i-1,j}}{(\Delta x)^2}\right), \quad i = 1,(M-1), j = 0,(N-1) \qquad (9)$$

$$u_{i,0} = \varphi(x_i), \qquad i = 0, M \qquad (10)$$

$$u_{0,j} = \mu_1(t_j), u_{M,j} = \mu_2(t_j), \qquad j = 0, N. \qquad (11)$$

equations (9)–(11) can be discretise in the difference equation form

$$-A_{j+1}u_{i-1,j+1} + (1 + 2A_{j+1})u_{i,j+1} - A_{j+1}u_{i-1,j+1} = A_j u_{i-1,j} + (1 - 2A_j)u_{i,j} + A_j u_{i-1,j} \qquad (12)$$

for i=0,M−1, j =0,N−1 where $A_j = (\Delta t)a_j/(2(\Delta x)^2)$. At each time step t_{j+1} for j= 0,N−1 using Dirichlet boundary conditions the above difference equation can be expressed as (M − 1) × (M − 1) system of linear equations take the form

$$Cu_{j+1} = Ku_j + b$$

where $u_{j+1} = (u_{1,j+1}, u_{2,j+1}, ..., u_{M-1,j+1})^T$ for j = 0, N, $b = (b_1, b_2, ..., b_{M-1})^T$, C and K are tridiagonal matrices.

An example, consider the direct problem (1)–(3) with h = T = 1, and

$$\varphi(x) = u(x,0) = \exp(x) + \cosh(x) \qquad (13)$$

$$\mu_1(t) = u(0,t) = 2\exp(t^3 + t) \qquad (14)$$

$$\mu_2(t) = u(1,t) = (\exp(1) + \cosh(1))\exp(t^3 + t) \quad (15)$$

$$a(t) = 2t^2 + 1. \quad (16)$$

The true solution is given by

$$u(x,t) = (\exp(x) + \cosh(x))\exp(t^3 + t) \quad (17)$$

Figure 1 present the numerically obtained solution for *u(x,t)*. This figure indicates that an excellent agreement with true solution.

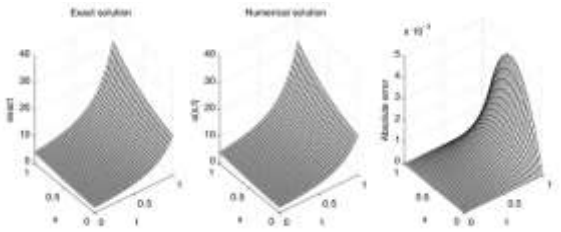

Figure 1*. the exact solution (left), numerical solution (middle), absolute error between them (right), for direct problem (1)-(3).*

On the other hand, outputs of interest equations (4) and (5), which are analytically given by

$$\mu_3(t) = (e + \sinh(1) - 1)\exp(t^3 + t), \quad t \in [0,1] \quad (18)$$

$$\mu_4(t) = (e + \sinh(1) - 1)\exp(t^3 + t), \quad t \in [0,1] \quad (19)$$

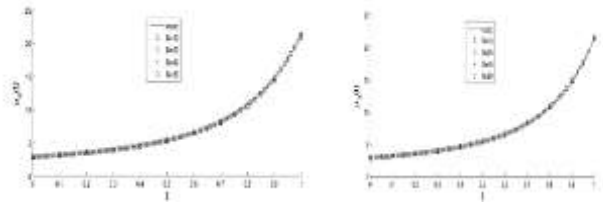

Figure 2. *The exact and numerical (left) $\mu_3(t)$ (right) $\mu_4(t)$ for M=N∈{10,20,40,80} for direct problem.*

Figure 2 explain that the true and numerical solutions for equations (4) and (5) are indistinguishable. The true solutions are given by equations (18) and (19), whilst the approximate results have been computed using the following second order finite-difference and trapezoidal rule formula.

$$\mu_3(t_j) = \int_0^1 u(x,t_j)dx = \frac{1}{2N}\left(\mu_1(t_j) + \mu_2(t_j) + 2\sum_{i=1}^{M-1} u_{i,j}\right), \quad j = 0,N \quad (20)$$

$$\mu_4(t_j) = \frac{4u_{M-1,j} - u_{M-2,j} - 3\mu_2(t_j)}{-2\,\Delta x} - \frac{4u_{1,j} - u_{2,j} - 3\mu_1(t_j)}{2\,\Delta x}, \quad j = 0,N, \quad (21)$$

To measure the accuracy of our numerical results, the root means square errors (*rmse*) between the numerical and the exact results for equations (4) and (5) are shown in the Table

M=N	10	20	40	80
$rmse(\mu_3)$	0.0243	0.0058	0.0014	3.2E-4
$rmse(\mu_4)$	0.2340	0.0562	0.0136	0.0033

1 which shows the mesh convergence,

$$rmse(\mu_k) = \sqrt{\frac{1}{N}\sum_{i=1}^{N}(\mu_k^{approx} - \mu_k^{exact})\text{^}2} \quad k = 3,4 \quad (22)$$

Table 1 *.The (rmse) given by (22), between the true and numerical solution for (4) and (5) for M=N ∈ {10,20,40,80} for direct problem (1)-(3).*

In this table it can be seen that as M = N increase the *rmse* values decrease indicating the mesh convergence.

4. Numerical solutions of the inverse problems

Suppose the coefficient a(t) > 0 is unknown, in this case we deal with inverse problem. To solve this, one can look at the quasi-solution [8], given by solving the minimization of the least-squares gap, for nonlinear ill-posed and inverse problem. We employ the Tikhonov regularization method based on minimizing the following functional;

$$F(a) = \left\| \int_0^h u(x,t)dx - \mu_3(t) \right\|^2 + \lambda||a||^2, \quad (23)$$

for IP1 and the corresponding functional for IP2 given by

$$G(a) = \|u_x(h,t) - u_x(0,t) - \mu_4(t)\|^2 + \beta||a||^2, \quad (24)$$

where u solves (1)–(4) or (1)–(3) and (5), respectively, $\lambda \geq 0$ and $\beta \geq 0$ are regularization parameters and the norm is usually the L^2 [0, T]-norm. The discrete form of the functionals (23) and (24) are;

$$F(\boldsymbol{a}) = \sum_{j=1}^{N}\left[\int_0^h u(x,t_j)dx - \mu_3(t_j)\right]^2 + \lambda\sum_{j=1}^{N} a_j^2, \quad (25)$$

$$G(\boldsymbol{a}) = \sum_{j=0}^{N}\left[u_x(h,t_j) - u_x(0,t_j) - \mu_4(t_j)\right]^2 + \beta\sum_{j=0}^{N} a_j^2, \quad (26)$$

Clearly if λ = β = 0, the above equations yield the ordinary least-squares methods which is usually produce unstable solution for noisy input data. It is worth to mention that, the minimization of *F* or *G* subject to the physical constraints that the thermal conductivity is positive quantity. The minimization processes are accomplished using the MATLAB routine *lsqnonlin* from optimization toolbox, [9]. This routine based on Trust-Region- Reflection (TRR) to find the local minimization of sums of squares functions starting from initial guess.

The needed parameters for the routine are taken as follows;

- Solution Tolerance (xTol)=10^{-10},
- Function Tolerance (FunTol)=10^{-10},
- Initial guess (a^0 = a(0)) for IP1 and IP2,
  The lower bound for a is 10^{-10} and the upper bound is 10^3.

5. Results and discussion

We discuss, in this section, a couple of test examples to illustrate the accuracy and stability of the numerical results. For simplicity, we take h = T = 1. In addition, we investigate the problems for exact and noisy inputs data. We add noise to the measured input data (4) and (5) as

$$\mu_3^{noise}(t_j) = \mu_3(t_j) + random('Normal', 0, \sigma_1, 1, N), \quad j = 1, N \qquad (27)$$

$$\mu_4^{noise}(t_j) = \mu_4(t_j) + random('Normal', 0, \sigma_1, 0, N), \quad j = 0, N \qquad (28)$$

where the *random* is a command in MATLAB which generates random variables by the Gaussian normal distribution with zero mean and standard deviation σ_1 and σ_2, computed as

$$\sigma_1 = p \times \max|\mu_3(t)|, \ \sigma_2 = p \times \max|\mu_4(t)|, \ t \in [0,T]. \qquad (29)$$

where p is the percentage of noise. In order to analyse the error between the exact and the numerical results, a similar formula of equations (22) will be used.

5.1 Example 1 for (IP1)

Consider the IP1 given by (1)–(4) with unknown coefficient *a(t)* and solve this inverse problem with measured input data (18). One can observe that the plot of the function $\mu'_1(t) + \mu'_2(t) = (2 + e + \cosh(1))(3t^2 + 1)\exp(t^3 + t)$ does not vanish over the time interval [0,1] and hence the unique solvability guaranteed by Theorem 1. The analytical solution for this problem is given by equations (16) and (17) and it can be verified by direct substitution. Also, the direct problem (1)–(3) corresponding to current example has been previously solved numerically using FDM in Section 3.

Let us begin with the case of no noise contaminated in the input data (4). The naive objective function (unregularized); i.e, $\lambda = 0$, as a function of the number of iterations is plotted in Figure 3 for various mesh parameters. From this figure and Table 2 it can be notice that the unregularized objective function (25) decreases rapidly to a very low value of order about $O(10^{-24})$ in 7 iterations. The numerical solution for the corresponding coefficient a(t) is shown in Figure 4. From this figure, one can notice that as M = N increase, a better result we obtain, the rmse values decrease, indicating that we achieve mesh independence and excellent agreement are obtained.

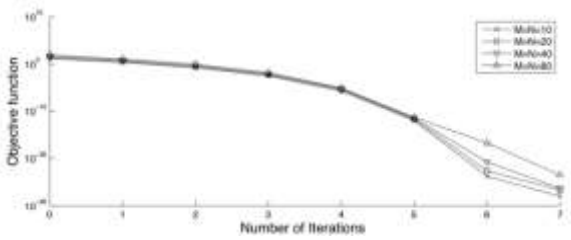

***Figure 3**. The unregularized objective function (25) with no noise, for various mesh size, for Example 1.*

Table 2. Number of iterations, number of function evaluations, value of objective function (25) at final iteration and the rmse values with no regularization and no noise for Example 1.

	M=N=10	M=N=20	M=N=40	M=N=80
No. of iteration	7	7	7	7
No. of function evaluations	96	176	336	656
Value of objective function (25) at final iteration	1.1E-28	2.2E-27	5.1E-27	3.4E-24
rmse(a)	0.2308	0.0548	0.0107	0.0024

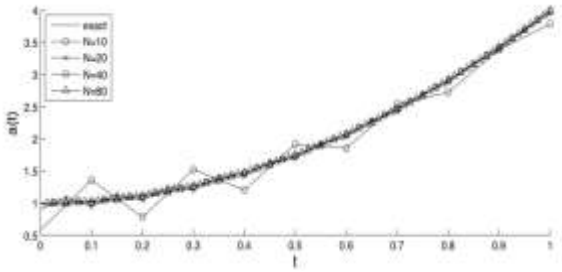

***Figure 4.** The coefficient a(t) for Example 1, with no noise and without regularization.*

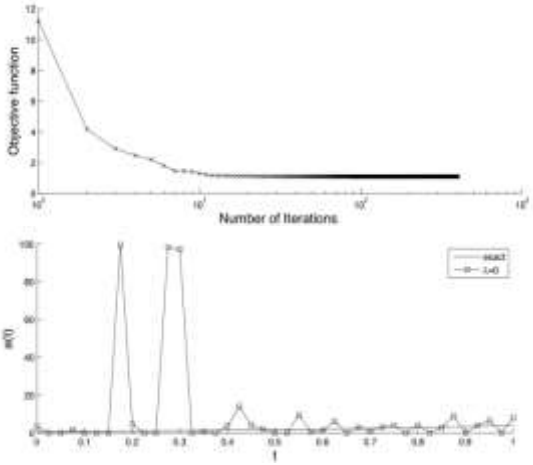

***Figure 5.** (up) the objective function (25) and (down) the coefficient a(t) for Example 1, with p=1% noise and without regularization.*

Next, let us fix the mesh parameter M = N = 40, for reasonable time consuming and add p = 1% noise to the measured input data $\mu_3(t)$ as given by (27). Figure 5 present the numerical results for the case of no regularization employed. From this figure it can be seen that the objective function (25) decreasing in slow manner whilst the unknown coefficient is unstable and unbounded solution. This behaviour is expected since the problem under investigation is ill-posed. Therefore, Tikhonov type regularization should be applied in order to retrieve the stability. The L-curve criteria [10] employed in order to choose an appropriate regularization parameter $\lambda > 0$ (for IP1) or $\beta > 0$ (for IP2), as shown in Figure 6(a), where the residual norm is $||\int_0^1 u(x,t)dx - \mu_3(t)||$.

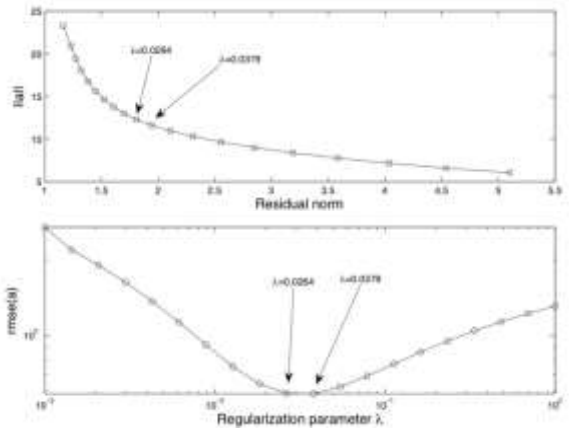

Figure 6. *(up)The residual norm versus the solution norm for the L-curve with various regularization parameters, and (down) The regularization parameters versus the rmse vales for the coefficient a(t), for Example 1 with p = 1% noise.*

Also, from this Figure 6, it can be seen that the two regularization parameter values located near the corner of the L-curve are $\lambda = \{0.0264, 0.0379\}$. These meet the minimum values of the *rmse* curve plotted versus regularization parameters in Figure 6(b). The associated numerical retrievals for the unknown a(t) when the two values of λ are selected are presented in Figure 7.

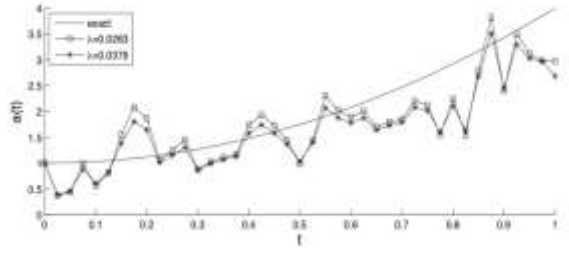

Figure 7. The numerical reconstructions for a(t) for Example 1, with p=1% noise.

From this figure, one can easily notice that as the regularization parameters $\lambda = 0.0379$ a better solution obtained see (-∗-) line. Moreover, the numerical solution for the temperature are depicted in Figure 8. From this figure, it can be seen that stable and accurate solutions are obtained. Also, it reported but not included that the same behaviour it can be seen for higher noise levels such as p = {3,5}%.

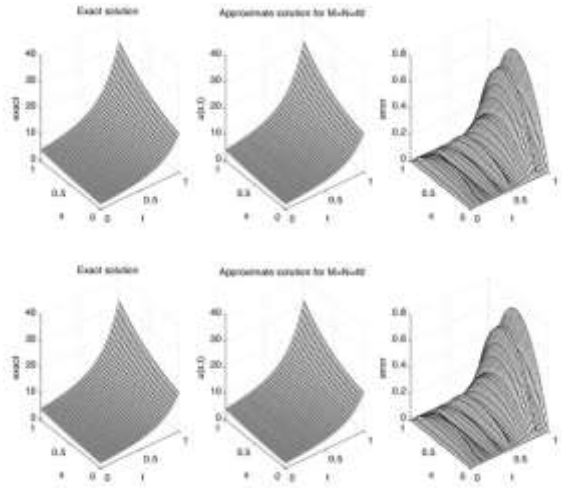

Figure 8*. The exact and numerical solutions and the absolute error between them when (up) $\lambda = 0.0264$ and (down) $\lambda = 0.0379$, for Example 1, with p = 1% noise.*

5.2 Example 2 for (IP2)

Now, we consider the inverse problem (1)–(3) and (5) with the unknown coefficient a(t) and solve this problem with the same data as in Example 1, but notice the difference for equation (4), the integral type, replaced by (5), which is the difference of heat fluxes.

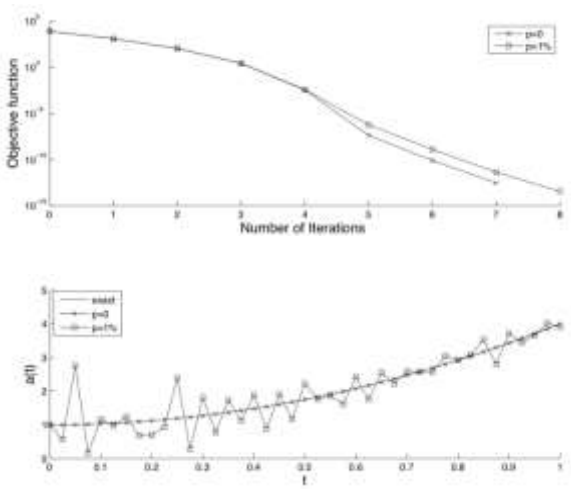

Figure 9*. (up) The unregularized objective function (26), i.e, $\beta = 0$, and (down) The exact and numerical solution for a(t), for Example 2, with p ∈{0,1}% level.*

As we notice that in previous example we can find the numerical solution for the temperature related with each noise percentage. Also, it is reported in this case we can obtain stable and accurate solutions when we apply regularization as we did in Example 1. Therefore, the results associated with regularization part has been omitted.

6. Conclusions

Two inverse coefficient identification problems have been numerically investigated. The finite difference method has been used in order to solve the direct problem. Whilst inverse problem recast as a nonlinear optimization problem which solved using MATLAB optimization toolbox. The numerical results are presented and it found accurate and stable.

References

[1] S. I. Kabanikhin. Definitions and examples of inverse and ill-posed problems. Journal of Inverse and Ill-Posed Problems, 16(4):317–357, 2008.

[2] M.S. Hussein, D. Lesnic, and M. Ivanchov. Free boundary determination in nonlinear diffusion. East Asian journal on applied mathematics, 3(4):295–310, 2013.

[3] M.S. Hussein, D. Lesnic, M.I. Ivanchov, and H.A. Snitko. Multiple time-dependent coefficient identification thermal problems with a free boundary. Applied Numerical Mathematics, 99:24–50, 2016.

[4] M.S. Hussein and D. Lesnic. Simultaneous determination of time-dependent coefficients and heat source. International Journal for Computational Methods in Engineering Science and Mechanics, 17(5-6):401–411, 2016.

[5] K. W. Morton and D. F. Mayers. Numerical solution of partial differential equations: an introduction. Cambridge university press, 2005.

[6] M.S. Hussein, D. Lesnic, and M.I. Ismailov. An inverse problem of finding the time- dependent diffusion coefficient from an integral condition. Mathematical Methods in the Applied Sciences, 39(5):963–980, 2016.

[7] N.I. Ivanchov. Inverse problems for the heat-conduction equation with nonlocal boundary conditions. Ukrainian Mathematical Journal, 45(8):1186–1192, 1993.

[8] M.S. Hussein. Coefficient Identification Problems in Heat Transfer. PhD thesis, University of Leeds, 2016.

[9] Mathwoks. Documentation optimization toolbox, www.mathworks.com, September 2012.

[10] Per Christian Hansen. Analysis of discrete ill-posed problems by means of the L- curve. SIAM review, 34(4):561–580, 1992.